

# Frictional Behavior of Carbon Film Embedded with Controlling-Sized Graphene Nanocrystallites

Cheng Chen · Dongfeng Diao · Xue Fan ·  
Lei Yang · Chao Wang

Received: 31 March 2014 / Accepted: 1 July 2014 / Published online: 16 July 2014  
© Springer Science+Business Media New York 2014

**Abstract** Graphene nanocrystallites embedded in amorphous carbon matrix can bring excellent tribological, electrical and magnetical properties to the carbon films. But too large size of graphene nanocrystallite would lead to degradation of the tribological performance. So it is necessary to clarify the dependence of frictional behavior of the carbon film on graphene nanocrystallite size. In order to control the size, different electron irradiation densities were introduced during film growth in the electron cyclotron resonance plasma sputtering process. Frictional tests on the films were carried out with a Pin-on-Disk tribometer. The evolution of graphene nanocrystallite size along with electron irradiation density was examined by transmission electron microscopy and Raman spectroscopy. The results showed that the graphene nanocrystallite size increased with increasing of the electron irradiation density. The film with a graphene nanocrystallite size of 1.09 nm exhibited a low friction coefficient of 0.03 and a long wear life. When nanocrystallite size increased, the friction coefficient increased and the wear life decreased. Observation on transfer film revealed that the nanocrystallite in transfer film grew larger when initial size was 1.09 nm, and changed smaller when initial size was 1.67 nm. The results suggested that embedded graphene nanocrystallite played an important role in the formation of transfer film, the initial size of graphene nanocrystallite

strongly affected the frictional behavior of the film, and the graphene nanocrystallite needed to be controlled under a certain size in order to keep the good tribological performance.

**Keywords** Carbon film · Graphene nanocrystallite · Electron irradiation · Frictional behavior · Transfer film

## 1 Introduction

Carbon films embedded with nanocrystallites, for example graphite, fullerene, nanotubes and diamonds, have attracted much attention because when the nanocrystallites are embedded in the amorphous carbon matrix, the excellent characteristics of the nanocrystallites enhance the overall properties of the films. It has been reported that carbon film embedded with oriented graphitic sheets showed outstanding directional thermal and electrical properties [1]. Amorphous carbon film containing fullerene clusters exhibited a high hardness, high elastic recovery [2, 3] and ultralow friction coefficient [4]. When carbon nanotubes were embedded in an amorphous carbon matrix, the field emission current [5], elastic modulus [6] and wear resistance [7, 8] can be increased. Diamond nanocrystallites can enhance the tribological properties of the carbon film with impressively low friction and wear [9, 10]. Recently, we proposed a low-energy electron irradiation technique in electron cyclotron resonance (ECR) plasma to prepare graphene nanocrystallite-embedded carbon film, which has a similar  $\pi$  electronic structure to that of bilayer graphene [11]. Graphene nanocrystallite-embedded carbon film shows outstanding electric properties and paramagnetic behavior, indicating that it has potential for electronic and spintronic applications [12]. For tribological application,

C. Chen · X. Fan · L. Yang  
Key Laboratory of Education Ministry for Modern Design and Rotor-Bearing System, Xi'an Jiaotong University, Xi'an 710049, China

D. Diao (✉) · C. Wang  
Institute of Nanosurface Science and Engineering (INSE), Shenzhen University, Shenzhen 518060, China  
e-mail: dfdiao@szu.edu.cn

the graphene nanocrystallite-embedded carbon films not only exhibit the potential to achieve low friction at the early stage of sliding contact [13, 14], but also have a high tribological thermostability [15]. These excellent characteristics of the films are mainly attributed to the features of graphene nanocrystallites. It is well known that the low friction performance of graphene or graphite is derived from the weak van der Waals bond force between graphene sheets [16, 17]. However, it has also been noted that when the size of the graphene nanocrystallite is too large or the overall structure of the carbon film is graphite, the weak bond force between graphene sheets also results in a dramatic degradation of the tribological performance [15, 18, 19]. This demonstrates that the tribological performance of the carbon film is closely related to the size of graphene nanocrystallite. However, the dependence of the frictional behavior of the carbon film on graphene nanocrystallite size is not clear.

In this study, in order to understand the effect of graphene nanocrystallite size on the friction behavior, different electron irradiation densities were introduced as a method to control the graphene nanocrystallite size during film growth in the ECR plasma sputtering process. Detailed investigations of graphene nanocrystallite sizes of the films have been carried out to reveal the role of graphene nanocrystallite in transfer film formation and low friction behavior.

## 2 Experiments

### 2.1 Film Fabrication

Carbon films were deposited on silicon substrates (p-type <100>) with electron irradiation using an ECR plasma sputtering system. The detailed description of carbon film fabrication with electron irradiation was reported in our previous works [11, 13], which is illustrated in Fig. 1. Electrons were resonantly accelerated to move around the magnetic field lines, and their momentums at the magnetic mirror position (dashed lines in Fig. 1) were zero. Then, electron irradiation was realized by applying a positive bias voltage on the substrate, which was located close to the magnetic mirror position. Silicon substrates were cut into  $20 \times 20$  mm squares and were fixed onto the substrate holder after cleaning in acetone and an ethanol bath by ultrasonic wave. The background pressure of the vacuum chamber was  $3 \times 10^{-4}$  Pa, and argon was inflated to keep the working pressure at  $4 \times 10^{-2}$  Pa. Before deposition, the substrates were cleaned by argon ion sputtering for 3 min. Then, argon ions sputtered the carbon target with a bias voltage of  $-300$  V to provide carbon atoms for the film growth. During deposition, a low-energy (50 eV)

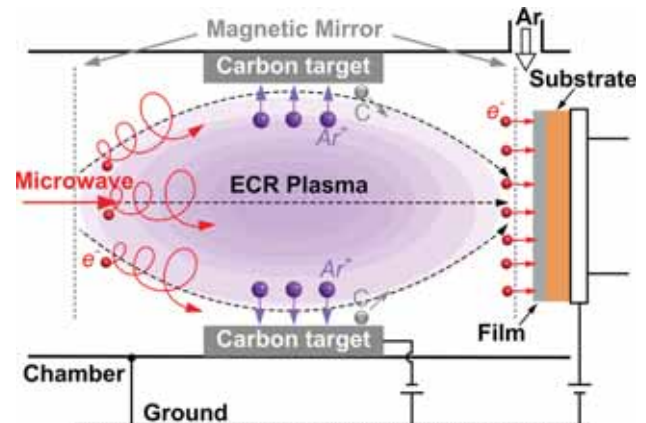


**Fig. 1** Schematic illustration of carbon film fabrication with electron irradiation [11]

electron irradiation was realized by applying a positive bias voltage of 50 V to the substrate [13]. Microwave power was used to adjust the ionization proportion of argon gas. A high ionization proportion means high ion and electron densities. Microwave power was set at 160, 200 and 300 W to obtain the electron irradiation densities of 30, 65 and 100 mA/cm<sup>2</sup>, respectively. The corresponding film growth rates were 4, 8.5 and 13 nm/min. The film thicknesses were about 200 nm. The substrate temperature rose from room temperature to 140–300 °C depending on different electron irradiation densities; the substrate temperature increased as the electron irradiation density increased, which was measured by a thermal couple fixed behind the substrate holder.

### 2.2 Nanostructural and Tribological Characterizations

The graphene nanocrystallites were observed with a JEM-2100 transmission electron microscope (TEM) operated at 200 kV. Samples for plan view were prepared by scratching the film surface with a diamond pencil, then transferring the flakes onto a copper micro grid. Samples for the cross-sectional view were prepared by conventional mechanical polishing followed by ion beam milling. The sizes of graphene nanocrystallites in carbon films were measured with Raman spectroscopy. Raman spectra between 1,100 and 3,500 cm<sup>-1</sup> were obtained with a HORIBA HR800 laser confocal Raman spectrometer using a 514 nm laser for excitation. The surface morphologies were measured by atomic force microscopy (AFM) with a scanning size of  $5 \times 5$  μm.

Frictional tests of the films sliding against a Si<sub>3</sub>N<sub>4</sub> ball (radius of 3.17 mm) were performed with a Pin-on-Disk tribometer. The surface roughness of the Si<sub>3</sub>N<sub>4</sub> ball was 3.33 nm measured by AFM. The normal load was 2 N. The sliding velocity was 26.4 mm/s, corresponding to a

constant disk rotational speed of 180 rpm with a frictional radius of 1.4 mm. The tests were operated at room temperature and a relative humidity of 40–60 %. The worn surface morphologies after 5,000 sliding cycles were measured with AFM. The structures of the worn scars on the Si<sub>3</sub>N<sub>4</sub> ball surfaces were observed and analyzed with an optical microscope and Raman spectroscopy.

### 3 Results

#### 3.1 Characterization of Graphene Nanocrystallite Sizes

Figure 2 shows the TEM images of the carbon films fabricated with different electron irradiation densities. As shown in Fig. 2a, when carbon film was fabricated with an electron irradiation density of 30 mA/cm<sup>2</sup>, graphene nanocrystallites were distributed uniformly in the amorphous carbon matrix. The orientation of graphene sheets was perpendicular to the substrate in the cross-sectional

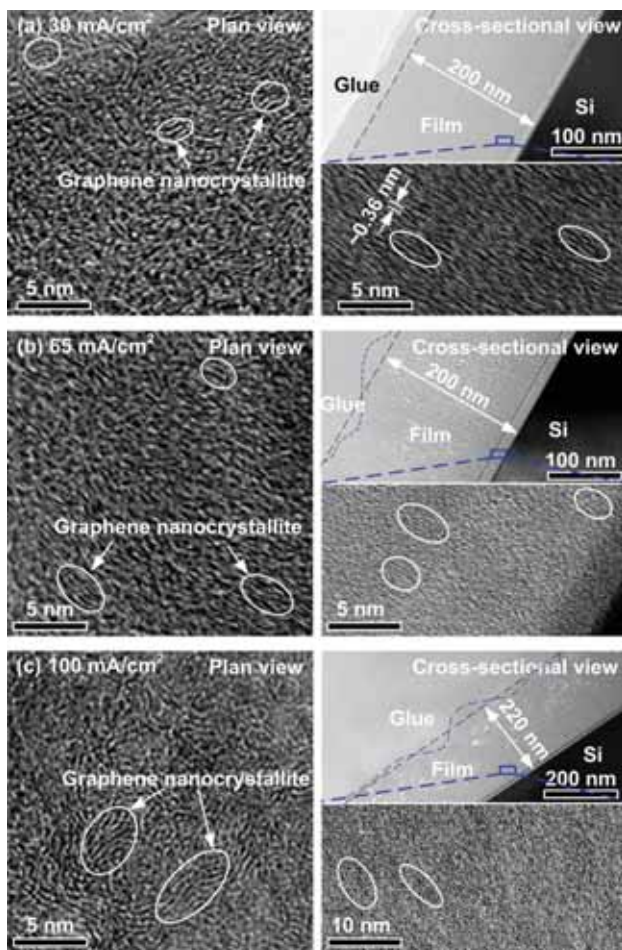


**Fig. 2** TEM images of the carbon films fabricated with electron irradiation densities of **a** 30 mA/cm<sup>2</sup>, **b** 65 mA/cm<sup>2</sup> and **c** 100 mA/cm<sup>2</sup>

plane. The interplanar spacing of graphene sheets was approximately 0.36 nm. The size of graphene nanocrystallite was about 1–2 nm. The film thickness was 200 nm. When electron irradiation density increased to 65 and 100 mA/cm<sup>2</sup>, as shown in Fig. 2b, c, the graphene nanocrystallite size increased slightly and the film surfaces became rougher, which will be further discussed in the following results. The corresponding film thicknesses were 200 and 220 nm.

Raman spectroscopy was used to analyze the variation of graphene nanocrystallite size, and the spectra are shown in Fig. 3. Each spectrum consists of a D band, G band and 2D band around 1,340, 1,590 and 2,700 cm<sup>-1</sup>, respectively. The shape of the three bands became sharper as the electron irradiation density increased, implying that the structure of the carbon film became more graphene-like. The D band and G band were fitted with a Lorentzian line and a Breit-Fano-Wagner (BFW) line, respectively. The Raman spectra results are summarized in Table 1, where a blue shift in the G band position and an increase in the I<sub>D</sub>/I<sub>G</sub> ratio can be observed with the increasing of electron

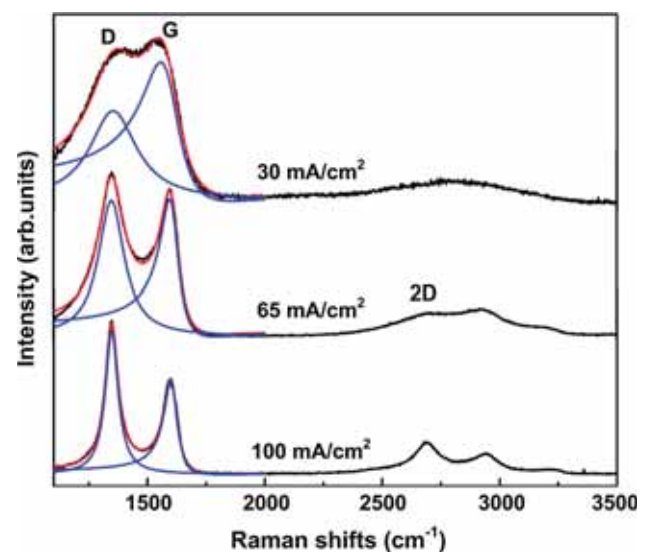


**Fig. 3** Raman spectra of the carbon films fabricated with different electron irradiation densities (*black curves*). *Blue curves*: D band and G band; *red curves*: fitting result (color figure online)

**Table 1** Raman spectra results of the carbon films fabricated with different electron irradiation densities

Sample	1	2	3
Irradiation density (mA/cm <sup>2</sup> )	30	65	100
G band position (cm <sup>-1</sup> )	1,547.1	1,592.9	1,598.8
I <sub>D</sub> /I <sub>G</sub>	0.65	0.99	1.54
L <sub>α</sub> (nm)	1.09	1.34	1.67

irradiation density. According to the three-stage amorphization [20], the carbon films fabricated with different electron irradiation densities are in stage 2, ranging from amorphous carbon type to nanocrystalline graphite type. The in-plane size of graphene nanocrystallite ( $L_x$ ) can be estimated with the equation:

$$I_D/I_G = C(\lambda) \cdot L_x^2 \quad (1)$$

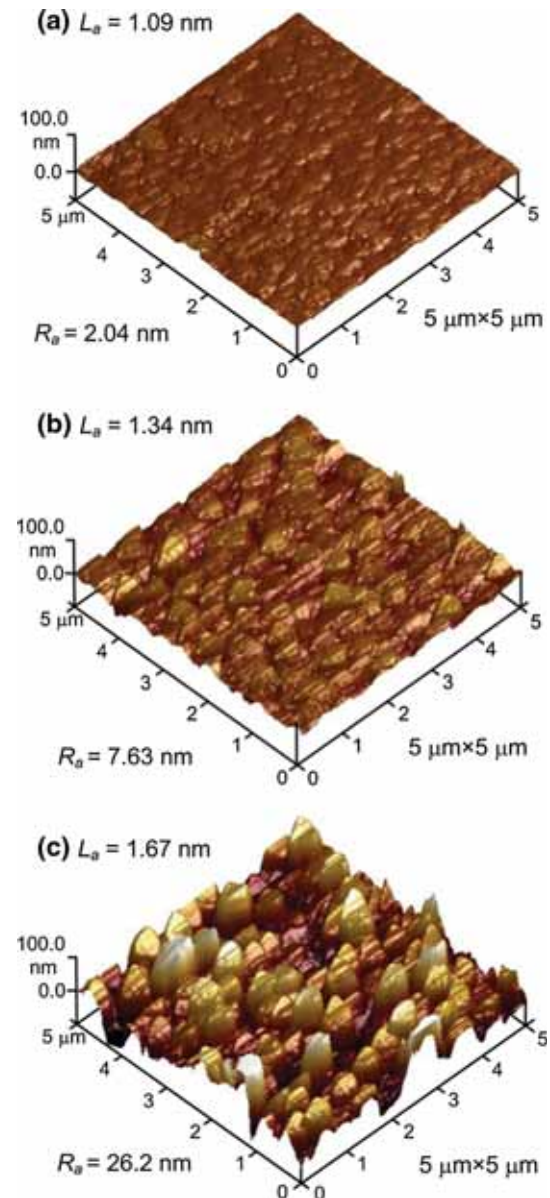
where  $C(\lambda)$  is the coefficient related to excitation laser wavelength. In this study,  $C(\lambda = 514 \text{ nm})$  is  $0.55 \text{ nm}^{-2}$ . The calculated graphene nanocrystallite sizes are also shown in Table 1. With the electron irradiation densities of 30, 65 and  $100 \text{ mA/cm}^2$ , the graphene nanocrystallite sizes were 1.09, 1.34 and 1.67 nm, respectively, suggesting that the graphene nanocrystallite size increased with the electron irradiation density. The graphene nanocrystallite size observed in TEM is slightly larger than that calculated from the Raman spectrum. This is because the graphene nanocrystallite size calculated from the Raman spectrum is an average value. During the film growth, the electrons (50 eV) could exchange sufficient energy with carbon atoms through inelastic scattering, which brings about the transformations from  $sp^3$  bonds to  $sp^2$  bonds and the formation of graphene nanocrystallites [11]. When the electron irradiation density increased, the energy exchanging process between electrons and carbon atoms was more intense and efficient. As a result, more carbon atoms would be excited to bond with each other in  $sp^2$  carbon hybridization, which could be the reason for the increase of the graphene nanocrystallite size.

### 3.2 Surface Morphologies

Figure 4 shows the surface morphologies of the carbon films. For the film with a graphene nanocrystallite size of 1.09 nm, the surface was smooth with a mean surface roughness ( $R_a$ ) of 2.04 nm, as shown in Fig. 4a. When the sizes were 1.34 and 1.67 nm, the surface roughnesses increased to 7.63 and 26.2 nm, and numerous micro asperities with radius of hundreds of nanometers appeared on the surfaces, as shown in Fig. 4b, c. It has been reported that the formation of the  $sp^2$  cluster leads to surface roughening [18, 21]. In this study, during the film growth, the electrons (50 eV) were not effective in smoothing the surface through the displacement of the carbon atom. Therefore, the surface roughness increased with increasing graphene nanocrystallite size.

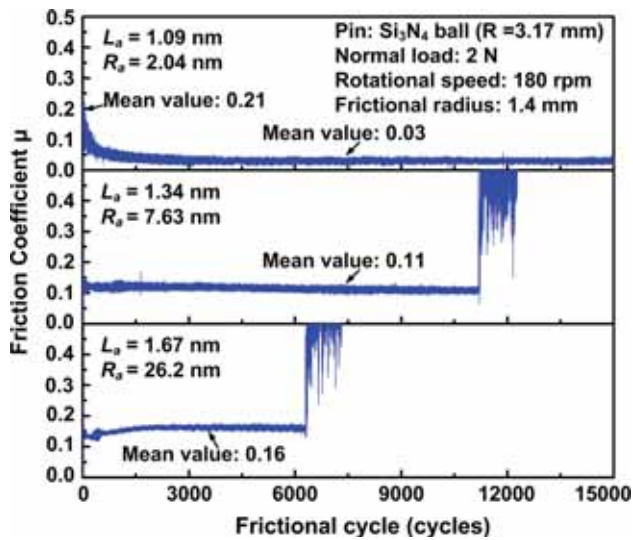
### 3.3 Frictional Behaviors

Figure 5 shows the typical friction curves of the carbon films embedded with different graphene nanocrystallite sizes. The friction coefficient of the film with a graphene



**Fig. 4** Surface morphologies of the carbon films with graphene nanocrystallite sizes of **a** 1.09 nm, **b** 1.34 nm and **c** 1.67 nm

nanocrystallite size of 1.09 nm was about 0.21 at the beginning and decreased to a lower value of 0.03 after about 1,000 sliding cycles. The low friction stage was stable and wear life of the carbon film was more than 15,000 cycles. For the films with graphene nanocrystallite sizes of 1.34 and 1.67 nm, the friction coefficients stayed constant with mean values of 0.11 and 0.16 from the beginning of the tests. Then, the friction coefficients showed sudden rises after about 11,100 and 6,300 sliding cycles, respectively. The sudden rises in the friction coefficient were caused by the failure of the films. Although the film with graphene nanocrystallite size of 1.67 nm was about 20 nm thicker than those of the others, the wear life



**Fig. 5** Friction curves of the carbon films with different graphene nanocrystallite sizes

of the film was the shortest. The above results indicate that the friction coefficient increased and wear life decreased with the increasing of graphene nanocrystallite size.

### 3.4 Structures of Transfer Films

In order to understand the frictional behaviors of the carbon films, the structures of worn scars on the  $\text{Si}_3\text{N}_4$  ball surfaces after 5,000 sliding cycles were observed and analyzed with an optical microscope and Raman spectroscopy. The results are shown in Fig. 6. From the optical images, transfer films can be found on the counter sliding surfaces of  $\text{Si}_3\text{N}_4$  balls for all three carbon films. Similarly, the graphene nanocrystallite sizes in the transfer films ( $L_{a,t}$ ) were estimated from the Raman spectra and are indicated in Fig. 6. Since transfer film thickness was not uniform at the surface of  $\text{Si}_3\text{N}_4$  balls, in order to accurately measure the nanocrystallite size in the transfer film, at least six positions were chosen to perform the test, especially at the positions with different transfer film thicknesses; three representative positions are marked in Fig. 6. The deviation of  $L_{a,t}$  was from measurements of the transfer film at different positions. For the film with a graphene nanocrystallite size of 1.09 nm,  $L_{a,t}$  ( $1.34 \pm 0.01$  nm) was larger than  $L_a$ , as shown in Fig. 6a, implying that “graphenization” occurred on the counter sliding surfaces, which could also be the reason for the decrease in the friction coefficient during sliding (see Fig. 5) [14, 22]. For the film with a graphene nanocrystal size of 1.34 nm,  $L_{a,t}$  ( $1.35 \pm 0.01$  nm) was almost equal to  $L_a$ , as shown in Fig. 6b. The further increase in the graphene nanocrystallite size of carbon film to 1.67 nm,  $L_{a,t}$  ( $1.50 \pm 0.10$  nm) became smaller than  $L_a$  (1.67 nm), as shown in Fig. 6c.

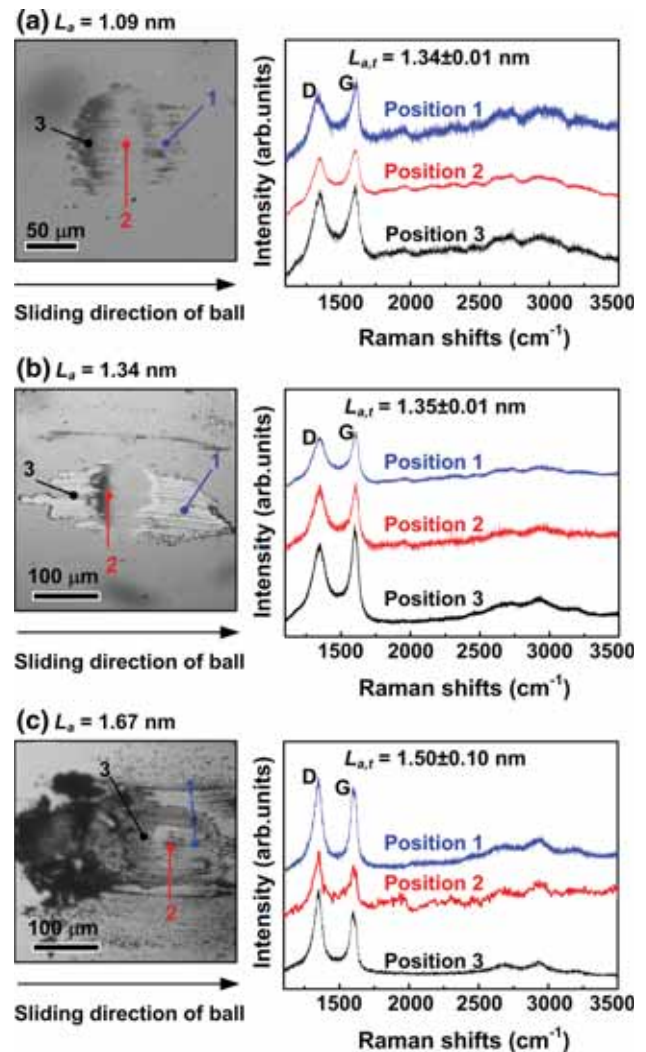


**Fig. 6** Optical images and Raman analysis of the worn scars on the  $\text{Si}_3\text{N}_4$  ball surfaces after 5,000 sliding cycles of the carbon films with graphene nanocrystallite sizes of **a** 1.09 nm, **b** 1.34 nm and **c** 1.67 nm. The corresponding graphene nanocrystallite sizes in the transfer films ( $L_{a,t}$ ) were calculated and are indicated in the figure. The deviation of  $L_{a,t}$  was from measurements of the transfer film at different positions

The above results imply that the  $L_{a,t}$  increased with the increasing of  $L_a$ . Also, friction did not always give rise to an increase in the graphene nanocrystallite size under such sliding conditions.

### 3.5 Worn-surface Morphologies

The worn-surface morphologies of the carbon films after 5,000 sliding cycles were measured with AFM. The results are shown in Fig. 7. It can be seen that the surface roughnesses of the three films decreased a lot after sliding. The surface of the film with graphene nanocrystallite size of 1.09 nm became very smooth, as shown in Fig. 7a. However, for the films with graphene nanocrystallite sizes

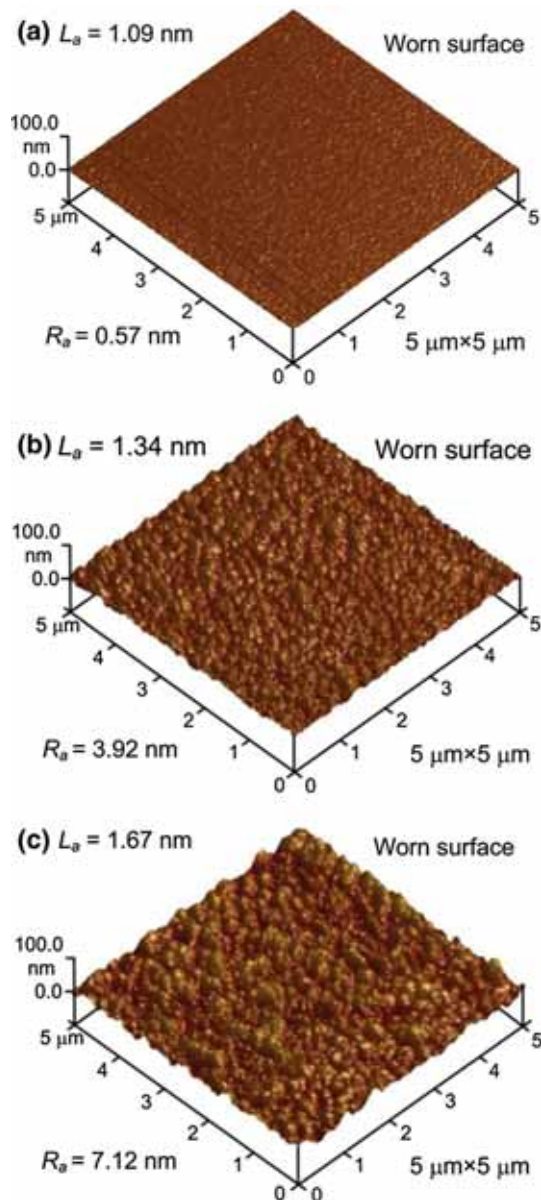


**Fig. 7** Worn surface morphologies of the carbon films with initial graphene nanocrystallite sizes of **a** 1.09 nm, **b** 1.34 nm and **c** 1.67 nm after 5,000 sliding cycles

of 1.34 nm and 1.67 nm, the surfaces were still very rough, as shown in Fig. 7b, c.

#### 4 Discussion

In order to understand the effect of graphene nanocrystallite size on the frictional behavior of carbon film, a description was proposed and is illustrated in Fig. 8. For the carbon film with a graphene nanocrystallite size of 1.09 nm, a transfer film formed on the counter sliding surface of the  $\text{Si}_3\text{N}_4$  ball with wear debris of the carbon

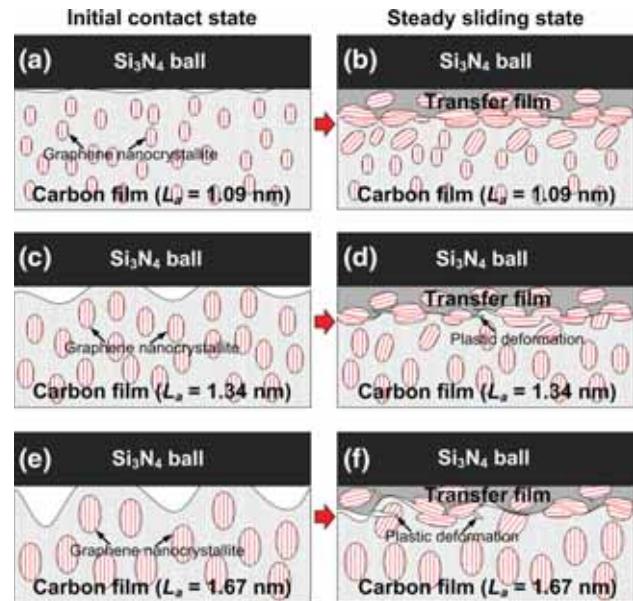


**Fig. 8** Illustration of the graphene nanocrystallite size effect on the frictional behavior of the graphene nanocrystallite-embedded carbon film. Initial contact states of carbon films with graphene nanocrystallite sizes of **a** 1.09 nm, **c** 1.34 nm and **e** 1.67 nm. Steady sliding states of carbon films with graphene nanocrystallite sizes of **b** 1.09 nm, **d** 1.34 nm and **f** 1.67 nm. Red line stands for the graphene sheet (color figure online)

film after sliding (see Fig. 8a, b). The size of graphene nanocrystallites in the transfer film increased, which may have been caused by sliding-induced heat [22] or shear-induced stress relaxation [23] at the contact region. Similarly, we can infer that the size of the graphene nanocrystallites in the contact surface of the carbon film may also increase. During the sliding shear process, the graphene sheets would lay parallel to the sliding direction. The presence of graphene sheets in the sliding surfaces changed the interactions between the sliding surfaces from strong covalent bonds to mainly weak van der Waal forces [24], leading to the friction coefficient decreasing and achieving a low value of 0.03 (see Fig. 5). For the film with a graphene nanocrystallite size of 1.34 nm, the graphene nanocrystallite size in the transfer film was almost equal to that in the original carbon film (see Fig. 8c, d). Therefore, the transfer film could easily form with the wear debris of the carbon film. This may be the reason why a steady friction stage could be achieved at the beginning of sliding contact (see Fig. 5). However, the surface of the film was very rough. After sliding, there were still many large asperities on the sliding surfaces, which could cause the occurrence of mechanical interlocking between surface asperities, resulting in plastic deformation of the asperities and an increase in the friction coefficient. When the graphene nanocrystallite size of the carbon film increased to 1.67 nm, the surface became rougher and the plastic

deformation of the asperities became more serious, leading to the decrease of graphene nanocrystallite size in sliding contact (see Fig. 8e, f). These caused the sharp degradation of the frictional performances of the film (see Fig. 5). Based on the above analysis, it can be inferred that the graphene nanocrystallite embedded in the carbon film played an important part in the formation of the transfer film and the initial size of the nanocrystallite strongly affected on the frictional behavior of the film.

## 5 Conclusion

The effect of graphene nanocrystallite size on the frictional behavior of carbon film fabricated with electron irradiation was studied. The graphene nanocrystallite size can be controlled by changing the electron irradiation density during film deposition. The carbon film with a graphene nanocrystallite size of 1.09 nm showed a low friction coefficient (0.03) and a long wear life. As the nanocrystallite size increased, the friction coefficient increased and the wear life decreased. The nanocrystallite in transfer film grew larger when the initial size was 1.09 nm and changed smaller when the initial size was 1.67 nm. Plastic deformation was considered to be the mechanism for the decrease in nanocrystallite size in sliding contact, which resulted in a high friction coefficient and fast wearing out of the film. This research demonstrated that embedded graphene nanocrystallite played an important role in the formation of the transfer film, and the initial size of the graphene nanocrystallite had a significant effect on the frictional behavior of the film. The graphene nanocrystallite should be controlled at a certain size in order to maintain good tribological performance.

**Acknowledgments** The authors would like to thank the National Nature Science Foundation of China, Grant Nos. 91323303 and 51175405.

## References

- Shakerzadeh, M., Loh, G.C., Xu, N., Chow, W.L., Tan, C.W., Lu, C., Yap, R.C.C., Tan, D., Tsang, S.H., Teo, E.H.T., Tay, B.K.: Re-ordering chaotic carbon: origins and application of textured carbon. *Adv. Mater.* **24**, 4112–4123 (2012)
- Wang, Q., Wang, C.B., Wang, Z., Zhang, J.Y., He, D.Y.: Fullerene nanostructure induced excellent mechanical properties in hydrogenated amorphous carbon. *Appl. Phys. Lett.* **91**, 141902 (2007)
- Alexandrou, I., Scheibe, H.J., Kiely, C.J., Papworth, A.J., Amarantunga, G.A.J., Schultrich, B.: Carbon films with an sp<sup>2</sup> network structure. *Phys. Rev. B* **60**, 10903 (1999)
- Wang, Z., Wang, C.B., Zhang, B., Zhang, J.Y.: Ultralow friction behaviors of hydrogenated fullerene-like carbon films: effect of normal load and surface tribochemistry. *Tribol. Lett.* **41**, 607–615 (2011)
- Zanin, H., May, P.W., Hamanaka, M.H.M.O., Corat, E.J.: Field emission from hybrid diamond-like carbon and carbon nanotube composite structures. *ACS Appl. Mater. Interfaces* **5**, 12238–12243 (2013)
- Fyta, M.G., Kelires, P.C.: Simulations of composite carbon films with nanotube inclusions. *Appl. Phys. Lett.* **86**, 191916 (2005)
- Li, L., Niu, J.B., Xia, Z.H., Yang, Y.Q., Liang, J.Y.: Nanotube/matrix interfacial friction and sliding in composites with an amorphous carbon matrix. *Scripta Mater.* **65**, 1014–1017 (2011)
- Lim, D.S., An, J.W., Lee, H.J.: Effect of carbon nanotube addition on the tribological behavior of carbon/carbon composites. *Wear* **252**, 512–517 (2002)
- Marciano, F.R., Costa, R.P.C., Lima-Oliveira, D.A., Lobo, A.O., Corat, E.J., Trava-Airoldi, V.J.: Tribological behavior under aggressive environment of diamond-like carbon films with incorporated nanocrystalline diamond particles. *Surf. Coat. Technol.* **206**, 434–439 (2011)
- Konicek, A.R., Grierson, D.S., Gilbert, P.U.P.A., Sawyer, W.G., Sumant, A.V., Carpick, R.W.: Origin of Ultralow Friction and Wear in Ultrananocrystalline Diamond. *Phys. Rev. Lett.* **100**, 235502 (2008)
- Wang, C., Diao, D.F., Fan, X., Chen, C.: Graphene sheets embedded carbon film prepared by electron irradiation in electron cyclotron resonance plasma. *Appl. Phys. Lett.* **100**, 231909 (2012)
- Wang, C., Diao, D.F.: Magnetic behavior of graphene sheets embedded carbon film originated from graphene nanocrystallite. *Appl. Phys. Lett.* **102**, 052402 (2013)
- Wang, C., Diao, D.F.: Cross-linked graphene layer embedded carbon film prepared using electron irradiation in ECR plasma sputtering. *Surf. Coat. Technol.* **206**, 1899–1904 (2011)
- Diao, D.F., Wang, C., Fan, X.: Frictional behavior of nanostructured carbon films. *Friction* **1**, 63–71 (2013)
- Chen, C., Diao, D.F.: Tribological thermostability of carbon film with vertically aligned graphene sheets. *Tribol. Lett.* **50**, 305–311 (2013)
- Lee, H., Lee, N., Seo, Y., Eom, J., Lee, S.: Comparison of frictional forces on graphene and graphite. *Nanotechnology* **20**, 325701 (2009)
- Dienwiebel, M., Verhoeven, G.S., Pradeep, N., Frenken, J.W.M., Heimberg, J.A., Zandbergen, H.W.: Superlubricity of graphite. *Phys. Rev. Lett.* **92**, 126101 (2004)
- Penkov, O.V., Pukha, V.E., Zubarev, E.N., Yoo, S.S., Kim, D.E.: Tribological properties of nanostructured DLC coatings deposited by C<sub>60</sub> ion beam. *Tribol. Int.* **60**, 127–135 (2013)
- Kataria, S., Dhara, S., Barshilia, H.C., Dash, S., Tyagi, A.K.: Evolution of coefficient of friction with deposition temperature in diamond like carbon thin films. *J. Appl. Phys.* **112**, 023525 (2012)
- Ferrari, A.C., Robertson, J.: Interpretation of Raman spectra of disordered and amorphous carbon. *Phys. Rev. B.* **61**, 14095–14106 (2000)
- Peng, X.L., Barber, Z.H., Clyne, T.W.: Surface roughness of diamond-like carbon films prepared using various techniques. *Surf. Coat. Technol.* **138**, 23–32 (2001)
- Donnet, C., Erdemir, A.: Tribology of diamond-like carbon films: Fundamentals and applications. In: Ronkainen, H., Holmberg, K. (eds.) *Environmental and thermal effects on the tribological performance of DLC coatings*, pp. 155–200. Springer, New York (2008)
- Ma, T.B., Hu, Y.Z., Wang, H.: Molecular dynamics simulation of shear-induced graphitization of amorphous carbon films. *Carbon* **47**, 1953–1957 (2009)
- Ma, T.B., Hu, Y.Z., Xu, L., Wang, L.F., Wang, H.: Shear-induced lamellar ordering and interfacial sliding in amorphous carbon films: a superlow friction regime. *Chem. Phys. Lett.* **514**, 325–329 (2011)